Austin Journal of Clinical Ophthalmology

Austin Publishing Group

Open Access Full Text Article

Review Article

The Development and Applications of Optical Coherence Tomography

Rimayanti U[1]*, Kiuchi Y[2] and Maulidia R[3]

[1]Department of Nursing, UIN Alauddin Makassar, Indonesia

[2]Department of Ophthalmology and Visual Science, Hiroshima University, Japan

[3]Department of Ophthalmology, Awal Bros Hospital, Indonesia

***Corresponding author:** Rimayanti U, Department of Nursing, Faculty of Health Sciences, UIN Alauddin Makassar, Jl. Sultan Alauddin 36, Samata, Gowa, 90222, Indonesia, Tel: +62-82190321230; Email: rimayantiu@gmail.com

Received: August 20, 2014; **Accepted:** September 15, 2014; **Published:** September 16, 2014

Abstract

Optical Coherence Tomography (OCT) was first applied for imaging of the eye, and until now, it has showed the largest benefit for ophthalmological examinations. The dynamic development of OCT has resulted in higher resolution, sensitivity, accuracy, and reproducibility of image of the detailed eye structures. This paper reviews the development of OCT and its applications to diagnose, monitor, and evaluate the treatment of eye diseases.

Keywords: Optical coherence tomography; Retina

Optical Coherence Tomography Development

Optical coherence tomography (OCT) is an emerging optical imaging technology that uses low-coherence light to perform high-resolution, cross-sectional imaging of the internal structure [1,2]. The imaging can be performed in-situ and in real time [3]. OCT was first applied for imaging of the eye, and recently, OCT has had the largest influence for clinical use in ophthalmology [4,5]. The reasons for that include the high transmittance of ocular media, the interferometric sensitivity and precision of OCT, which fits well the near-optical quality of many ophthalmological structures [6]. Thus, OCT has already become a routine tool for the investigation, mainly in the posterior segment of the eye. OCT can also be helpful to make the image of anterior part of eye, including details of corneal pathologies and structural changes of the chamber angle and iris [7,8].

OCT was first demonstrated by Huang D, et al. [1]. In 1993, the first *in vivo* tomograms of the human retina were published by Fercher et al. [9] and Swanson et al [10]. Initially, OCT techniques were based on low time-coherence interferometry (LCI) scans performed in the time domain [6]. Time-domain OCT (TD-OCT) generates cross-sectional images by measuring the echo time delay and intensity of light that is reflected or backscattered from intraocular structures [1]. To obtain the image of retinal layers, TD-OCT uses near-infrared light directed at the retina and also reflected from a reference mirror that is positioned at a known distance from each retinal layer. When light reflected from the retina combines with light reflected from the reference mirror, a pattern is formed. The reference mirror is then moved to different distances from the retina, thus producing different signals for the light reflected back from each respective retinal layer. A time delay is used to form a different signal (axial scan [A-scan]) for each retinal layer. Multiple A-scans are then combined to construct a two-dimensional image (B-scan) displaying a different signal for each retinal layer [11].

Two scans have to be performed in standard TD-OCT: the lateral OCT scan addresses laterally adjacent sample positions, and the OCT depth-scan to detect depth positions of light re-emitting sites in the sample [5]. The first commercially available OCT machine was the OCT 1000 marketed in 1996 by Carl Zeiss Meditec (Dublin, CA). The conventional TD-OCT system used moving reference mirror, which causes a physical constraint, provides imaging rate limited to approximately 400 A-scans per second, with an axial resolution of 10 μm [12]. Several improvements in OCT hardware have been introduced since the first commercial TD-OCT system became available. Better axial resolution [13-15] and increased scanning speed [16-22] are the two main advancements.

The advent of Spectral Domain OCT (SD-OCT) eliminated the need for the axial movement of the scanning mirror required in TD-OCT, yielding improved resolution and speed. The spectrometer-based SD-OCT, also known as Fourier domain OCT [23,24], uses a broadband light source and a low-loss spectrometer to measure the spectral oscillations from the different layers. SD-OCT obtains images by keeping the reference mirror in one position and collecting all of the backscattered light from the retina at a single point in time [25]. This technique relies on differences in the frequency spectrum of light reflected from the different layers [26].

Using the spectral technique, no OCT depth-scan is needed and, therefore, data acquisition can be very fast [6]. In a TDOCT system, increasing source bandwidth decreases the signal-to-noise ratio (SNR) as it requires increased electronic detection bandwidth, while the SNR of spectrally discriminated techniques in Fourier domain and swept source SD-OCT are independent of the source coherence length [25,27]. Therefore, both spectrometer- and swept source-based SDOCT systems show superior sensitivity advantage over the TD-OCT, leading to higher speed and scan. Current SD-OCT machines scan at up to 55,000 A-scans per second and provide an axial resolution lower than 5 μm [12,28].

Swept source-OCT (SS-OCT) obtains time-encoded spectral information by sweeping a narrow-bandwidth laser through a

Citation: Rimayanti U, Kiuchi Y and Maulidia R. The Development and Applications of Optical Coherence Tomography. Austin J Clin Ophthalmol. 2014;1(7): 1032.

Table 1: Comparison of Time-Domain Optical Coherence Tomography (TD-OCT), Spectral-Domain OCT, and Swept-Source OCT.

Parameter	TD-OCT	SD-OCT	SS-OCT
Working Principle	Measure the echo time delay and intensity of reflected light	Measure the wavelengths of reflected light	Measure the wavelengths of reflected light
Light Source	Broadband and continuous wave	Broadband and continuous wave	Narrow instantaneous line width, rapidly swept wave
Central Wavelength	830 nm	830 nm	1300 nm
Axial resolution/transverse resolution	~10 μm/20-25 μm	~5 to 7 μm/10-25 μm	~5 to 7 μm/~12.5 μm
Scan Speed	400 A-scans/second	~55,000 A-scans/second	~400,000 A-scans/second

broad optical spectrum. Backscattered intensity is detected with a photodetector. This process is in contrast to SD-OCT, which uses a broad bandwidth light source and detects the interference spectra with a charge-coupled device (CCD) camera and spectrometer [29]. SD-OCT has been commonly used, but there are some benefits of using SS-OCT compared to SD-OCT systems. One of them is that SS-OCT has greater sensitivity and lower signal-to-noise ratios (SNR) at greater scanning depths. Another advantage of SS-OCT is that it does not require a CCD camera and spectrometer. Therefore, the complexity is decreased and the CCD array cost is abolished. To date, speeds of up to 400,000 A-scans/s have been attained in the eye using the SS-OCT [30]. Thus, reducing sampling errors, potential motion artifact, and the possibility of missing focal pathologies. Most of the SS-OCT systems are now operating at 1–1.3 μm wavelengths, only few studies demonstrating SS-OCT in the 800 nm range [31,32]. The use of 1–1.3 μm wavelengths resulted in lower axial resolution but deeper penetration into the posterior segment of the eye [33,34]. The water absorption window at 1.3 μm offers even deeper penetration of light and may be useful for cornea and anterior segment imaging [35,36]. The illustration about the differences between TD-OCT, SD-OCT, and SS-OCT is shown in Table (1).

Current applications of optical coherence tomography in ophthalmology

Glaucoma: The most common scan patterns in TD-OCT glaucoma imaging were a 3.4 mm scan around the optic nerve head (ONH) and six equally spaced radial scans through the macula (6 mm) and optic nerve (4 mm) [29]. Retinal nerve fiber layer (RNFL) thickness is obtained via automated RNFL segmentation in the circumpapillary scan protocol. The segmentation of the RNFL is performed automatically by detecting the internal limiting membrane and outer RNFL border in each A-scan of OCT frame and calculated as the distance between these two boundaries [37]. SD-OCT produces an RNFL thickness map by acquiring a 6 × 6 mm cube of signal data in the peripapillary region in less than 1.5 seconds [38]. Each cube of data consists of data points, which will be compared with the signal from an age-matched normative database in a deviation map. A 3.46-mm peripapillary circle of data points centered on the optic disc is then extracted to construct a peripapillary RNFL map. This map displays mean absolute thickness measurements of the different peripapillary regions according to the corresponding quadrant or segment. Each segment is also color-coded according to the relative thickness in that area compared with the normative age-matched database. Red, yellow, and green colors represent a less than 1%, 1% to 5%, 5% to 95% amount that the measured RNFL thickness is within normal range for an age-matched population, respectively. A white color means the RNFL thickness is thicker than 95% of age-matched database [11].

Macular thickness (Internal Limiting Membrane [ILM] to the photoreceptor inner segment-outer [IS–OS] segment junction) is automatically segmented in the macular scan pattern. The optic nerve scan is used to obtain cup area, disc area, rim area, cup diameter, and disc diameter [29]. In subjects with ocular hypertension, retinal nerve fiber layer defects and normal visual fields, the vertical cup-to-disc diameter ratio, total neuroretinal rim area, rim-to-disc area ratio, and cup-to-disc area ratio are the most valuable optic disc variables for early detection of glaucomatous optic nerve damage [39]. Another study noted that global parameters, namely cup and rim area and horizontal cup-disc ratio, were less likely to detect early focal glaucomatous optic nerve head changes, than parameters representing localised changes, such as minimum rim width within the 60 degrees and 90 degrees sectors across the vertical meridian [40]. Neuroretinal rim area declined at the rate of between 0.28% and 0.39% per year, while vertical optic cup diameter, optic cup area, and mean cup/disc diameter ratio increased with age [41]. Thus, age-related changes should be taken into account when assessing glaucoma diagnosis and progression.

The ONH and RNFL scan protocols have been used since TD-OCT became commercially available, and RNFL and ONH parameters have been shown to be significantly different between glaucomatous and healthy eyes [42,43]. Measurement using TD-OCT showed that the glaucoma-discriminating ability of circumpapillary RNFL and optic nerve head parameters were higher than macular volume and thickness [44-46]. The higher speed and resolution of SD-OCT improved the repeatability of macular imaging compared to standard TD-OCT. The addition of macular ganglion cell complex (GCC) parameters to SD-OCT gives benefit for glaucoma diagnosis. One commercially available system (RTVue, Optovue, Inc) has developed an approach for summarizing GCC, which consists of the retinal ganglion layer (retinal ganglion cell bodies), retinal nerve fiber (RGC axons), and inner plexiform layers (RGC dendrites). The GCC measurements are then directly compared to a normative database. The SD-OCT GCC average had significantly higher diagnostic power than macular retinal thickness measured by SD-OCT and TD-OCT in differentiating between perimetric glaucoma and normal groups [47]. Two of the GCC pattern parameters, GLV and FLV, sum up the volume of GCC loss in the macula with differing levels of locality. The Global Loss Volume (GLV) measures the average amount of GCC volume loss over the entire GCC field, while the Focal Loss Volume (FLV) is used to detect focal losses to correct for overall absolute changes [48]. FLV and GLV were found to have higher diagnostic accuracy than the simple average for the diagnosis of perimetric glaucoma [47-50]. The GCC, FLV, and GLV measured using RTVue is presented in Figure 1.

Retina: The measurement of OCT is very important in the

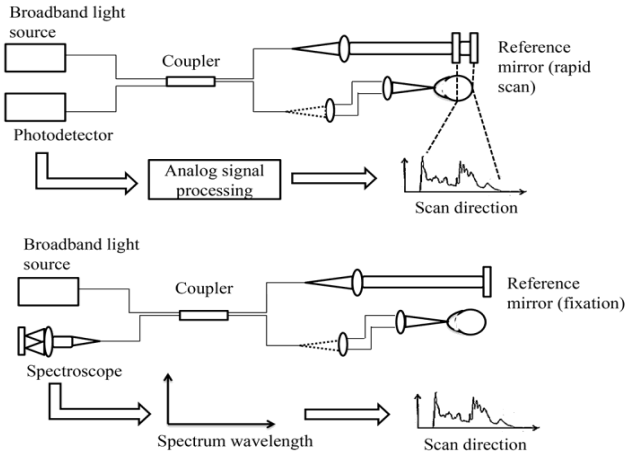

Figure 1: Schematic drawing of TD-OCT and SD-OCT systems.

diagnosis, management, and evaluation of retinal diseases. The TD -OCT system provides a macular scan pattern which is derived from 6 radial B-scans crossing at the fovea. By interpolating data from these scans, the average macular thickness is calculated in 9 subfields centered on the fovea. The total macular volume is obtained using a similar method [51]. The SD-OCT provides images with much higher resolution, allowing the separation of the outer photoreceptor segments from the Retinal Pigment Epithelium (RPE) and their inclusion in the calculation of the retinal thickness [52]. In contrast, using TD-OCT, the outer segments of the photoreceptors are not differentiated from the RPE, thus being excluded from the retinal thickness evaluation. This leads to significantly higher results of the average retinal thickness compared to those measured by TD-OCT [53].

Age-related Macular Degeneration (AMD) is the one of the diseases that undoubtedly had benefit from the development of the OCT technology. OCT demonstrated its usefulness in better understanding the pathogenesis of this disease. For the dry AMD, the same scan pattern can be used to image both drusen and Geographic Atrophy (GA). Reproducible, quantitative data on both the area of GA and the morphologic features of drusen can also be obtained. Another advantage of using OCT is that the same scan pattern can be used to image both drusen and geographic atrophy (GA) while obtaining reproducible, quantitative data on both the area of GA and the morphologic features of drusen [54]. The possibility to precisely measure the drusen volume with the support of the computer-assisted techniques offers a very useful possibility to monitor the disease and to assess the progression of drusen to both GA and choroidal neovascularization [52]. OCT instruments establish the prognostic criteria and evaluate the response to the treatment with anti-vascular endothelial growth factors in the wet form of the disease. Retinal thickening is determined by the exudation from the choroidal new vessels, while the occult choroidal neovascularization is revealed by the presence of the elevation, detachment or various alterations of the RPE [51]. Subretinal fluid, sub retinal tissue, and pigment epithelial detachments (PEDs) are all well visualized on OCT B-scans and have allowed the study of the anatomic features of CNV lesions [55]. PED with subretinal fluid accumulation visualized with OCT is shown in Figure 2.

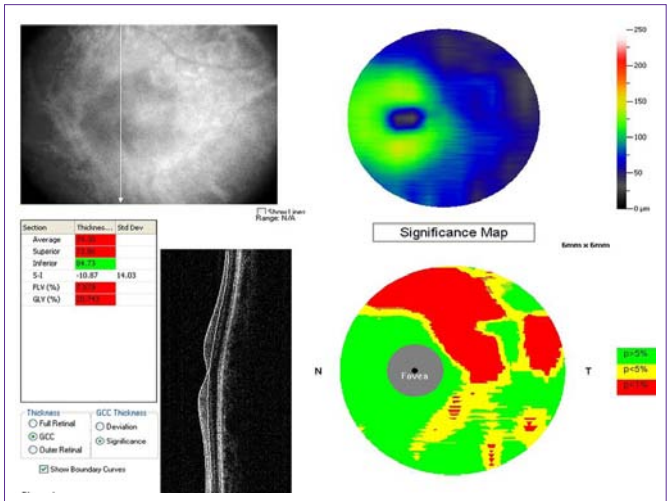

Figure 2: A patient with early glaucoma showed the superior GCC thinning, significant FLV and GLV values measured using RTVue SD-OCT.

The SD-OCT system allows the improvement of the detection and follow-up of retinal diseases, due to its ultrahigh-speed scan rate, superior axial and lateral resolutions, cross-sectional two-dimensional scan, and three-dimensional (3D) raster scan. An OCT fundus image [53,56], visualization and measurement of intraretinal layers such as photoreceptor, ganglion cell, plexiform, and nuclear layers [57,58] Scan be obtained using 3D OCT data. This OCT fundus image enables precise and reproducible cross-sectional OCT images. It is possible to acquire high-density volumetric data of the macula or optic disc. Therefore, 3D OCT data can be processed to provide comprehensive structural information about the retina [22]. The use of 3D scan also provides objective measurements before and after surgery. The imaging was used to visualize the vitreomacular interface in patients who were undergoing surgery for epiretinal membrane [59]. For post-surgery evaluation, the 3D imaging was performed for the photoreceptor IS–OS junctions observation as an indicator of visual outcomes after macular hole surgery [60,61]. Studies on the analysis of the vitreomacular interface have renewed our understanding of several maculopathies, such as idiopathic macular whole and diabetic macular edema. For example, a high prevalence of perifoveal posterior vitreous detachment with incomplete foveolar attachment has been demonstrated in diabetic patients with macular edema, suggesting a possible role of the vitreomacular interface status in the pathogenesis of diabetic macular edema [62].

Diabetic Macular Edema (DME) evaluation using OCT is associated with the prognosis of this disease. Kim et al. [63] used OCT to evaluate various morphologic patterns and investigated their relationship with visual acuity. The OCT patterns containing cystoid macular edema and posterior hyaloidal traction, and increasing retinal thickness in all patterns were significantly associated with worse vision. Cclassifying DME structural patterns using OCT might also allow the prediction of visual outcome after laser photocoagulation [64].

OCT-measured center point thickness measurement is also a useful tool for the detection and monitoring of macular edema in retinal vein occlusion, even though it cannot reliably substitute for visual acuity measurements [65]. A study using TD-OCT found that

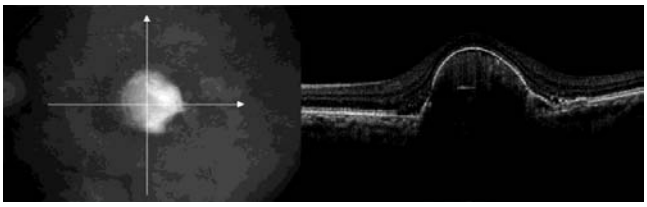

Figure 3: SD-OCT demonstrates a pigment epithelial detachment with subretinal fluid accumulation.

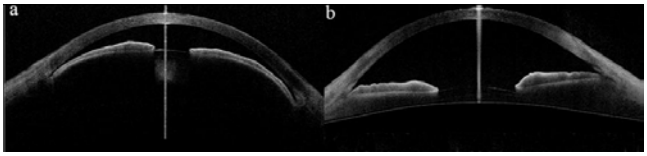

Figure 4: This figure shows a comparison between narrow (a) and normal (b) anterior chamber.

at month 3 treatment of anti-vascular endothelial growth factor, ranibizumab, OCT images provide predictive information for patients with central vein retinal occlusion, but not for those with branch retinal vein occlusion [66]. Currently, exact measurement of macular edema in retinal vein occlusion is available using optical coherence tomography (OCT). The latest generation of spectral-domain OCT enables a very accurate measurement of retinal volume in the macular region and its exact re measurement in follow-up visits. This information is superior to the fluorescein angiography findings and facilitates the evaluation of treatment response [67]. The loss of foveal photoreceptor inner segment/outer segment junction line and inner retinal layers on SD-OCT is significantly correlated with poorer visual outcomes in patients with central retinal vein occlusion [68].

Anterior segment: In 2001, Radhakrishnan et al. described the use of OCT for the anterior segment imaging [69]. They used an optical amplifier light source at a wavelength of 1310 nm to make an image of which the angle configuration and the scleral spur were clearly visible. Figure (3) shows the narrow and normal angles of anterior chamber.

The use of a longer wavelength laser of 1,310 nm from 830-nm wavelength was found to result in better penetration through structures with irregular surface [70,71]. That system has been adopted in commercially available anterior segment OCT systems. Geerling et al. [72] performed the anterior segment imaging using a commercially available 1,310-nm TD-OCT system (4Optics, Lübeck, Germany) with a dielectrical mirror to a surgical microscope. They concluded that this modification is particularly helpful for lamellar dissection surgery techniques such as deep anterior lamellar keratoplasty and trabeculectomy. In regard to the applications of anterior segment-OCT in the evaluation of IOP control after glaucoma surgery, an estimation of the value of IOP seems to be possible through the quantitative study of the reflectivity of the filtering bleb [73]. OCT also has a potential in the study of tear film behavior and in the diagnosis of dry eye. This may be the first application of OCT to obtain not only morphological, but also functional information of the ocular surface through an enhancement imaging [74-73].

The first ultrahigh resolution images of the human cornea *in vivo* were obtained using the Spectral OCT laboratory system with a super continuum light source [77]. Imaging of the anterior segment with high resolution Spectral OCT has been proven useful in diagnosis of the corneal pathologies and monitoring of cornea during its postoperative recovery [78-80]. Spectral OCT also allows high-resolution, cross-sectional visualization of the eye fitted with contact lens, as well as diagnosis, evaluation and documentation of contact lens complications [81].

Conclusion

The development of OCT has been significantly improving the understanding, diagnosis, and follow-up of eye diseases. The higher speed and resolution of OCT improved the accuracy and repeatability of macular imaging. Using three-dimensional OCT data, an OCT fundus image, visualization and measurement of intraretinal layers, objective measurements before and after surgery, thus providing comprehensive structural information about the retina. Imaging of the anterior segment with high-resolution OCT has been proven useful in diagnosis and monitoring of anterior segment of the eye. Some limitations appeared during the development of OCT, but its future is encouraging.

References

1. Huang D, Swanson EA, Lin CP, Schuman JS, Stinson WG, Chang W, et al. Optical coherence tomography. Science. 1991; 254: 1178-1181.
2. Fujimoto JG. Optical coherence tomography. Applied Physics. 2001; 4: 1099-1111.
3. Fujimoto JG, Pitris C, Boppart SA, Brezinski ME. Optical coherence tomography: an emerging technology for biomedical imaging and optical biopsy. Neoplasia. 2000; 2: 9-25.
4. Swanson EA, Izatt JA, Hee MR, Huang D, Lin CP, Schuman JS, et al. *In vivo* retinal imaging by optical coherence tomography. Opt Lett. 1993; 18: 1864-1866.
5. Fercher AF, Hitzenberger CK, Drexler W, Kamp G, Sattmann H. *In vivo* optical coherence tomography. Am J Ophthalmol. 1993; 116: 113-114.
6. Fercher AF, Drexler W, Hitzenberger CK, Lasser T. Optical coherence tomography—principles and applications. Rep Prog Phys. 2003; 66: 239–303.
7. Radhakrishnan S, Rollins AM, Roth JE, Yazdanfar S, Westphal V, Bardenstein DS, et al. Real-time optical coherence tomography of the anterior segment at 1310 nm. Arch Ophthalmol. 2001; 119: 1179-1185.
8. Hoerauf H, Birngruber R. Handbook of Optical Coherence Tomography. Tearney GJ, Bouma BE, editors. New York: Marcel Dekker. 2002.
9. Fercher AF, Hitzenberger CK, Drexler W, Kamp G, Sattmann H. *In vivo* optical coherence tomography. Am J Ophthalmol. 1993; 116: 113-114.
10. Swanson EA, Izatt JA, Hee MR, Huang D, Lin CP, Schuman JS, et al. *In vivo* retinal imaging by optical coherence tomography. Opt Lett. 1993; 18: 1864-1866.
11. Aref AA, Budenz DL. Spectral domain optical coherence tomography in the diagnosis and management of glaucoma. Ophthalmic Surg Lasers Imaging. 2010; 41: S15-S27.
12. Hahn P, Migacz J, O`Connell R, Maldonado RS, Izatt JA, Toth CA. The use of optical coherence tomography in intraoperative ophthalmic imaging. Ophthalmic Surg Lasers Imaging. 2011; 42: S85-S94.
13. Drexler W, Morgner U, Kärtner FX, Pitris C, Boppart SA, Li XD, et al. *In vivo* ultrahigh-resolution optical coherence tomography. Opt Lett. 1999; 24: 1221-1223.
14. Unterhuber A, Povazay B, Bizheva K, Hermann B, Sattmann H, Stingl A, et al. Advances in broad bandwidth light sources for ultrahigh resolution optical coherence tomography. Phys Med Biol. 2004; 49: 1235-1246.

15. Lim H, Jiang Y, Wang Y, Huang YC, Chen Z, Wise FW. Ultrahigh-resolution optical coherence tomography with a fiber laser source at 1 microm. Opt Lett. 2005; 30: 1171-1173.

16. Fercher A, Hitzenberger C, Kamp G, Elzaiat S. Measurement of intraocular distances by backscattering spectral interferometry. OptCommun. 1995; 117: 43–48.

17. Leitgeb R, Wojtkowski M, Kowalczyk A, Hitzenberger CK, Sticker M, Fercher AF. Spectral measurement of absorption by spectroscopic frequency-domain optical coherence tomography. Opt Lett. 2000; 25: 820-822.

18. Wojtkowski M, Leitgeb R, Kowalczyk A, Bajraszewski T, Fercher AF. *In vivo* human retinal imaging by Fourier domain optical coherence tomography. J Biomed Opt. 2002; 7: 457-463.

19. de Boer JF, Cense B, Park BH, Pierce MC, Tearney GJ, Bouma BE. Improved signal-to-noise ratio in spectral-domain compared with time-domain optical coherence tomography. Opt Lett. 2003; 28: 2067-2069.

20. Nassif N, Cense B, Park BH, Yun SH, Chen TC, Bouma BE, et al. *In vivo* human retinal imaging by ultrahigh-speed spectral domain optical coherence tomography. Opt Lett. 2004; 29: 480-482.

21. Choma MA, Hsu K, Izatt JA. Swept source optical coherence tomography using an all-fiber 1300-nm ring laser source. J Biomed Opt. 2005; 10: 44009.

22. Wojtkowski M, Srinivasan V, Fujimoto JG, Ko T, Schuman JS, Kowalczyk A, et al. Three-dimensional retinal imaging with high-speed ultrahigh-resolution optical coherence tomography. Ophthalmology. 2005; 112: 1734-1746.

23. Leitgeb R, Hitzenberger C, Fercher A. Performance of fourier domain vs. time domain optical coherence tomography. Opt Express. 2003; 11: 889-894.

24. Wojtkowski M, Kowalczyk A, Targowski P, Gorczynska I. Fourier-domain optical coherence tomography: next step in optical imaging. OpticaApplicata. 2002; 32: 569-580.

25. Yaqoob Z, Wu J, Yang C. Spectral domain optical coherence tomography: a better OCT imaging strategy. Biotechniques. 2005; 39: S6-13.

26. Fujimoto JG. Optical coherence tomography for ultrahigh resolution in vivo imaging. Nat Biotechnol. 2003; 21: 1361-1367.

27. Choma M, Sarunic M, Yang C, Izatt J. Sensitivity advantage of swept source and Fourier domain optical coherence tomography. Opt Express. 2003; 11: 2183-2189.

28. Schuman JS. Spectral domain optical coherence tomography for glaucoma (an AOS thesis). Trans Am Ophthalmol Soc. 2008; 106: 426-458.

29. Gabriele ML, Wollstein G, Ishikawa H, Kagemann L, Xu J, Folio LS, et al. Optical coherence tomography: history, current status, and laboratory work. Invest Ophthalmol Vis Sci. 2011; 52: 2425-2436.

30. Potsaid B, Baumann B, Huang D, Barry S, Cable AE, Schuman JS, et al. Ultrahigh speed 1050nm swept source/Fourier domain OCT retinal and anterior segment imaging at 100,000 to 400,000 axial scans per second. Opt Express. 2010; 18: 20029-20048.

31. Srinivasan VJ, Adler DC, Chen Y, Gorczynska I, Huber R, Duker JS, et al. Ultrahigh-speed optical coherence tomography for three-dimensional and en face imaging of the retina and optic nerve head. Invest Ophthalmol Vis Sci. 2008; 49: 5103-5110.

32. Lim H, Mujat M, Kerbage C, Lee EC, Chen Y, Chen TC, et al. High-speed imaging of human retina *in vivo* with swept-source optical coherence tomography. Opt Express. 2006; 14: 12902-12908.

33. Lee EC, de Boer JF, Mujat M, Lim H, Yun SH. *In vivo* optical frequency domain imaging of human retina and choroid. Opt Express. 2006; 14: 4403-4411.

34. Povazay B, Hermann B, Unterhuber A, Hofer B, Sattmann H, Zeiler F, et al. Three-dimensional optical coherence tomography at 1050 nm versus 800 nm in retinal pathologies: enhanced performance and choroidal penetration in cataract patients. J Biomed Opt. 2007; 12: 041211.

35. Yun S, Tearney G, de Boer J, Iftimia N, Bouma B. High-speed optical frequency-domain imaging. Opt Express. 2003; 11: 2953-2963.

36. Yasuno Y, Madjarova VD, Makita S, Akiba M, Morosawa A, Chong C, et al. Three-dimensional and high-speed swept-source optical coherence tomography for in vivo investigation of human anterior eye segments. Opt Express. 2005; 13: 10652-10664.

37. Gabriele ML, Ishikawa H, Wollstein G, Bilonick RA, Kagemann L, Wojtkowski M, et al. Peripapillary nerve fiber layer thickness profile determined with high speed, ultrahigh resolution optical coherence tomography high-density scanning. Invest Ophthalmol Vis Sci. 2007; 48: 3154-3160.

38. Leung CK, Lam S, Weinreb RN, Liu S, Ye C, Liu L, et al. Retinal nerve fiber layer imaging with spectral-domain optical coherence tomography: analysis of the retinal nerve fiber layer map for glaucoma detection. Ophthalmology. 2010; 117: 1684-1691.

39. Jonas JB, Bergua A, Schmitz-Valckenberg P, Papastathopoulos KI, Budde WM. Ranking of optic disc variables for detection of glaucomatous optic nerve damage. Invest Ophthalmol Vis Sci. 2000; 41: 1764-1773.

40. Gundersen KG, Heijl A, Bengtsson B. Sensitivity and specificity of structural optic disc parameters in chronic glaucoma. Acta Ophthalmol Scand. 1996; 74: 120-125.

41. Garway-Heath DF, Wollstein G, Hitchings RA. Aging changes of the optic nerve head in relation to open angle glaucoma. Br J Ophthalmol. 1997; 81: 840-845.

42. Mistlberger A, Liebmann JM, Greenfield DS, Pons ME, Hoh ST, Ishikawa H, et al. Heidelberg retina tomography and optical coherence tomography in normal, ocular-hypertensive, and glaucomatous eyes. Ophthalmology. 1999; 106: 2027-2032.

43. Pieroth L, Schuman JS, Hertzmark E, Hee MR, Wilkins JR, Coker J, et al. Evaluation of focal defects of the nerve fiber layer using optical coherence tomography. Ophthalmology. 1999; 106: 570-579.

44. Wollstein G, Ishikawa H, Wang J, Beaton SA, Schuman JS. Comparison of three optical coherence tomography scanning areas for detection of glaucomatous damage. Am J Ophthalmol. 2005; 139: 39-43.

45. Medeiros FA, Zangwill LM, Bowd C, Vessani RM, Susanna R Jr, Weinreb RN. Evaluation of retinal nerve fiber layer, optic nerve head, and macular thickness measurements for glaucoma detection using optical coherence tomography. Am J Ophthalmol. 2005; 139: 44–55.

46. Ojima T, Tanabe T, Hangai M, Yu S, Morishita S, Yoshimura N. Measurement of retinal nerve fiber layer thickness and macular volume for glaucoma detection using optical coherence tomography. Jpn J Ophthalmol. 2007; 51: 197-203.

47. Tan O, Chopra V, Lu AT, Schuman JS, Ishikawa H, Wollstein G, et al. Detection of macular ganglion cell loss in glaucoma by Fourier-domain optical coherence tomography. Ophthalmology. 2009; 116: 2305-2314.

48. Arintawati P, Sone T, Akita T, Tanaka J, Kiuchi Y. The applicability of ganglion cell complex parameters determined from SD-OCT images to detect glaucomatous eyes. J Glaucoma. 2013; 22: 713-718.

49. Rimayanti U, Latief MA, Arintawati P, Akita T, Tanaka J, Kiuchi Y. Width of abnormal ganglion cell complex area determined using optical coherence tomography to predict glaucoma. Jpn J Ophthalmol. 2014; 58: 47-55.

50. Rimayanti U, Kiuchi Y, Yamane K, Latief MA, Mochizuki H, Hirata J, et al. Inner retinal layer comparisons of eyes with exudative age-related macular degeneration and eyes with age-related macular degeneration and glaucoma. Graefes Arch Clin Exp Ophthalmol. 2014; 252: 563-570.

51. Talu SD, Talu S. Use of OCT Imaging in the Diagnosis and Monitoring of Age Related Macular Degeneration. Gui-Shuang Ying, editor. In: Age Related Macular Degeneration - The Recent Advances in Basic Research and Clinical Care. Rijeka: InTech. 2012; 253-272.

52. Coscas G. Optical Coherence Tomography in Age-Related Macular Degeneration. Heidelberg: Springer Medizin Verlag. 2009.

53. Podoleanu AG, Seeger M, Dobre GM, Webb DJ, Jackson DA, Fitzke FW. Transversal and longitudinal images from the retina of the living eye using low coherence reflectometry. J Biomed Opt. 1998; 3: 12-20.

54. Yehoshua Z, Rosenfeld PJ, Gregori G, Penha F. Spectral domain optical coherence tomography imaging of dry age-related macular degeneration. Ophthalmic Surg Lasers Imaging. 2010; 41: S6-S14.

55. Liakopoulos S, Ongchin S, Bansal A, Msutta S, Walsh AC, Updike PG, et al. Quantitative optical coherence tomography findings in various subtypes of neovascular age-related macular degeneration. Invest Ophthalmol Vis Sci. 2008; 49: 5048-5054.

56. Hitzenberger C, Trost P, Lo PW, Zhou Q. Three-dimensional imaging of the human retina by high-speed optical coherence tomography. Opt Express. 2003; 11: 2753-2761.

57. Drexler W, Morgner U, Ghanta RK, Kärtner FX, Schuman JS, Fujimoto JG. Ultrahigh-resolution ophthalmic optical coherence tomography. Nat Med. 2001; 7: 502-507.

58. Drexler W, Sattmann H, Hermann B, Ko TH, Stur M, Unterhuber A, et al. Enhanced visualization of macular pathology with the use of ultrahigh-resolution optical coherence tomography. Arch Ophthalmol. 2003; 121: 695-706.

59. Falkner-Radler CI, Glittenberg C, Binder S. Spectral domain high definition optical coherence tomography in patients undergoing epiretinal membrane surgery. Ophthalmic Surg Lasers Imaging. 2009; 40: 270–276.

60. Sano M, Shimoda Y, Hashimoto H, Kishi S. Restored photoreceptor outer segment and visual recovery after macular hole closure. Am J Ophthalmol. 2009; 147: 313-318.

61. Inoue M, Watanabe Y, Arakawa A, Sato S, Kobayashi S, Kadonosono K. Spectral-domain optical coherence tomography images of inner/outer segment junctions and macular hole surgery outcomes. Graefes Arch Clin Exp Ophthalmol. 2009; 247: 325-330.

62. Gaucher D, Tadayoni R, Erginay A, Haouchine B, Gaudric A, Massin P. Optical coherence tomography assessment of the vitreoretinal relationship in diabetic macular edema. Am J Ophthalmol. 2005; 139: 807-813.

63. Kim BY, Smith SD, Kaiser PK. Optical coherence tomographic patterns of diabetic macular edema. Am J Ophthalmol. 2006; 142: 405-412.

64. Kim NR, Kim YJ, Chin HS, Moon YS. Optical coherence tomographic patterns in diabetic macular oedema: prediction of visual outcome after focal laser photocoagulation. Br J Ophthalmol. 2009; 93: 901-905.

65. Scott IU, VanVeldhuisen PC, Oden NL, Ip MS, Blodi BA, Jumper JM, et al. SCORE Study report 1: baseline associations between central retinal thickness and visual acuity in patients with retinal vein occlusion. Ophthalmology. 2009; 116: 504-512.

66. Bhisitkul RB, Campochiaro PA, Shapiro H, Rubio RG. Predictive value in retinal vein occlusions of early versus late or incomplete ranibizumab response defined by optical coherence tomography. Ophthalmology. 2013; 120: 1057-1063.

67. Rehak M, Wiedemann P. Retinal vein thrombosis: pathogenesis and management. J Thromb Haemost. 2010; 8: 1886-1894.

68. Lima VC, Yeung L, Castro LC, Landa G, Rosen RB. Correlation between spectral domain optical coherence tomography findings and visual outcomes in central retinal vein occlusion. Clin Ophthalmol. 2011; 5: 299-305.

69. Radhakrishnan S, Rollins AM, Roth JE, Yazdanfar S, Westphal V, Bardenstein DS, et al. Real-time optical coherence tomography of the anterior segment at 1310 nm. Arch Ophthalmol. 2001; 119: 1179-1185.

70. Hoerauf H, Gordes RS, Scholz C, Wirbelauer C, Koch P, Engelhardt R, et al. First experimental and clini¬cal results with transscleral optical coherence tomography. Ophthalmic Surg Lasers. 2000; 31: 218-222.

71. Izatt JA, Hee MR, Swanson EA, Lin CP, Huang D, Schuman JS, et al. Micrometer-scale resolution imaging of the anterior eye *in vivo* with optical coherence tomography. Arch Ophthalmol. 1994; 112: 1584-1589.

72. Geerling G, Müller M, Winter C, Hoerauf H, Oelckers S, Laqua H, et al. Intraoperative 2-dimensional optical coherence tomography as a new tool for anterior segment surgery. Arch Ophthalmol. 2005; 123: 253-257.

73. Napoli PE, Zucca I, Fossarello M. Qualitative and quantitative analysis of filtering blebs with optical coherence tomography. Can J Ophthalmol. 2014; 49: 210-216.

74. Napoli PE, Satta GM, Coronella F, Fossarello M. Spectral-domain optical coherence tomography study on dynamic changes of human tears after instillation of artificial tears. Invest Ophthalmol Vis Sci. 2014; 55: 4533-4540.

75. Wang J, Simmons P, Aquavella J, Vehige J, Palakuru J, Chung S, et al. Dynamic distribution of artificial tears on the ocular surface. Arch Ophthalmol. 2008; 126: 619-625.

76. Napoli PE, Coronella F, Satta GM, Zucca IA, Fossarello M. A novel OCT technique to measure *in vivo* the corneal adhesiveness for sodium carboxymethylcellulose in humans and its validity in the diagnosis of dry eye. Invest Ophthalmol Vis Sci. 2014; 55: 3179-3185.

77. Wojtkowski M, Bajraszewski T, GorczyÅka I, Targowski P, Kowalczyk A, Wasilewski W, et al. Ophthalmic imaging by spectral optical coherence tomography. Am J Ophthalmol. 2004; 138: 412-419.

78. Kaluzny BJ, Kaluzny JJ, Szkulmowska A, Gorczynska I, Szkulmowski M, Bajraszewski T, et al. Spectral Optical Coherence Tomography: A Novel Technique for Cornea Imaging. Cornea. 2006; 25: 960-965.

79. Kaluzny BJ, Szkulmowska A, Szkulmowski M, Bajraszewski T, Wawrocka A, Krawczynski MR, et al. Granular corneal dystrophy in 830-nm spectral optical coherence tomography. Cornea. 2008; 27: 830-832.

80. Pang CE, M V, Tan DT, Mehta JS. Evaluation of Corneal Epithelial Healing Under Contact Lens with Spectral-Domain Anterior Segment Optical Coherence Tomography (SD-OCT). Open Ophthalmol J. 2011; 5: 51-54.

81. KaÅ, uzny BJ, Kaluzny JJ, Szkulmowska A, Gorczyńska I, Szkulmowski M, et al. Spectral optical coherence tomography: a new imaging technique in contact lens practice. Ophthalmic Physiol Opt. 2006; 26: 127-132.

Austin J Clin Ophthalmol - Volume 1 Issue 7 - 2014
ISSN : 2381-9162 | www.austinpublishinggroup.com

Citation: Rimayanti U, Kiuchi Y and Maulidia R. The Development and Applications of Optical Coherence Tomography. Austin J Clin Ophthalmol. 2014;1(7): 1032.